Regional coherence evaluation in mild cognitive impairment and Alzheimer's disease based on adaptively extracted magnetoencephalogram rhythms

2011 Physiol. Meas. 32 1163

(http://iopscience.iop.org/0967-3334/32/8/011)

IOP PUBLISHING PHYSIOLOGICAL MEASUREMENT

Physiol. Meas. **32** (2011) 1163–1180 doi:10.1088/0967-3334/32/8/011

Regional coherence evaluation in mild cognitive impairment and Alzheimer's disease based on adaptively extracted magnetoencephalogram rhythms

Javier Escudero[1,2,3], Saeid Sanei[2,4], Delaram Jarchi[2,4], Daniel Abásolo[3,5] and Roberto Hornero[3]

[1] Signal Processing and Multimedia Communication, School of Computing and Mathematics, University of Plymouth, Drake Circus, Plymouth PL4 8AA, UK
[2] Centre of Digital Signal Processing, Cardiff University, Cardiff CF24 3AA, UK
[3] Biomedical Engineering Group, University of Valladolid, Valladolid 47011, Spain
[4] Faculty of Electronic Engineering, Physics and Computing, University of Surrey, Guildford GU2 7XH, UK
[5] Centre for Biomedical Engineering, Division of Mechanical, Medical and Aerospace Engineering, University of Surrey, Guildford GU2 7XH, UK

E-mail: javier.escudero@ieee.org and javier.escudero@plymouth.ac.uk

Received 7 October 2010, accepted for publication 25 May 2011
Published 27 June 2011
Online at stacks.iop.org/PM/32/1163

Abstract

This study assesses the connectivity alterations caused by Alzheimer's disease (AD) and mild cognitive impairment (MCI) in magnetoencephalogram (MEG) background activity. Moreover, a novel methodology to adaptively extract brain rhythms from the MEG is introduced. This methodology relies on the ability of empirical mode decomposition to isolate local signal oscillations and constrained blind source separation to extract the activity that jointly represents a subset of channels. Inter-regional MEG connectivity was analysed for 36 AD, 18 MCI and 26 control subjects in δ, θ, α and β bands over left and right central, anterior, lateral and posterior regions with magnitude squared coherence—$c(f)$. For the sake of comparison, $c(f)$ was calculated from the original MEG channels and from the adaptively extracted rhythms. The results indicated that AD and MCI cause slight alterations in the MEG connectivity. Computed from the extracted rhythms, $c(f)$ distinguished AD and MCI subjects from controls with 69.4% and 77.3% accuracies, respectively, in a full leave-one-out cross-validation evaluation. These values were higher than those obtained without the proposed extraction methodology.

Keywords: Alzheimer's disease (AD), magnitude square coherence ($c(f)$), constrained blind source separation (cBSS), empirical mode decomposition (EMD), magnetoencephalogram (MEG), mild cognitive impairment (MCI)

1. Introduction

Alzheimer's disease (AD) is a neurodegenerative disorder. It causes memory loss and other cognitive and behavioural symptoms that progressively impair the daily activities (Blennow *et al* 2006, Nestor *et al* 2004). AD is the most common form of dementia in the western world. It accounts for 50–60% of all dementia cases (Blennow *et al* 2006). Its prevalence increases almost exponentially with age (Blennow *et al* 2006, Nestor *et al* 2004). As a consequence, AD is one of the most disabling and burdensome health conditions worldwide (Ferri *et al* 2006). A definite diagnosis of AD can only be made by necropsy (Blennow *et al* 2006). In clinical practice, AD is diagnosed based on the criteria set by McKhann *et al* (1984). Yet, the accuracy is limited (Blennow *et al* 2006). Hence, it is important to develop methods to help in AD diagnosis in order to improve the patients' care and allow more accurately targeted future therapies.

Mild cognitive impairment (MCI) shares some features with AD. The cognitive deficits of MCI subjects are limited to memory but their activities of daily living are preserved (Nestor *et al* 2004). Thus, this concept could represent a transitional period before full-blown dementia (Blennow *et al* 2006, Nestor *et al* 2004). The rate of conversion to AD is about ten times higher for MCI subjects than that for the general population. Yet, the narrow definition of MCI might fail to capture the heterogeneity of clinical AD (Nestor *et al* 2004).

Spectral (Abatzoglou *et al* 2009, Escudero *et al* 2009, Poza *et al* 2008, Rossini *et al* 2007) and nonlinear analysis techniques (Abásolo *et al* 2008, Abatzoglou *et al* 2007, Gómez *et al* 2009a, van Cappellen van Walsum *et al* 2003) have been applied to single channels of electroencephalogram (EEG) and magnetoencephalogram (MEG) recordings from AD patients. The general conclusion of those studies is that AD causes both a spectral slowdown and alterations in the nonlinear dynamics of the electromagnetic brain activity (Hornero *et al* 2009, Jeong 2004, Stam 2010). Additionally, AD can be characterized as a disconnection syndrome (Jeong 2004, Stam *et al* 2009, 2006). The brain activity has also been studied in MCI subjects (Babiloni *et al* 2006, Fernández *et al* 2006, Rossini *et al* 2008, 2006). Overall, differences are more easily found between healthy elderly subjects and AD patients than for MCI subjects (Jeong 2004, Stam 2010). This may be due to the small gap between the MCI subjects and the other two groups (Fernández *et al* 2006, Gómez *et al* 2009b). Given that MCI is considered as an intermediate state between healthy ageing and full-blown AD, MCI subjects might also show connectivity alterations in their brain recordings (Gómez *et al* 2009b). The connectivity of the electromagnetic brain activity might help to predict the development of AD in MCI subjects (Rossini *et al* 2006). Moreover, MEG has some desirable properties over the EEG when studying brain activity. MEG recordings are reference free and less affected by extra-cerebral tissues than EEG signals (Rossini *et al* 2007, Stam 2010).

Magnitude squared coherence—$c(f)$—is a widespread connectivity metric, which provides a measure of the linear dependences between two signals as a function of frequency (Dauwels *et al* 2010, Pereda *et al* 2005). It has been hypothesised that AD decreases $c(f)$ in α and β but there are no conclusive findings about the δ and θ bands (Jeong 2004, Rossini *et al* 2007). Furthermore, AD produces opposite changes in features computed from different spectral bands (Alonso *et al* 2011, Stam *et al* 2009, van Cappellen van Walsum *et al* 2003). Thus, it is advisable to analyse different spectral bands separately (Stam 2010).

Yet, $c(f)$ has several limitations. Firstly, spurious correlations could appear due to the volume conduction (Gómez *et al* 2009b, Nolte *et al* 2004, Stam *et al* 2009). This effect is due to the fact that nearby channels are likely to record activity from identical currents. This leads to abnormally high correlations in the results that reflect volume conduction rather than actual connectivity (Gómez *et al* 2009b, Nolte *et al* 2004, Stam *et al* 2009). Other alternatives, such

as the imaginary part of the coherency (Nolte *et al* 2004) or the phase lag index (Stam *et al* 2009), have been proposed. However, their use is much more limited and their interpretation is less straightforward than for $c(f)$ (Nolte *et al* 2004, Stam *et al* 2009). Furthermore, these measures are usually applied in a channel-wise manner, producing a very high number of variables (Dauwels *et al* 2010, Gómez *et al* 2009b). A possible option is to try to estimate the equivalent current dipoles (Hoechstetter *et al* 2004, Rossini *et al* 2007, Supp *et al* 2007). Once the currents have been estimated, the same connectivity metrics used in the channel-wise analyses can be applied to them. Moreover, the volume conduction effect does not affect these dipole-based connectivity assessments (Hoechstetter *et al* 2004, Supp *et al* 2007). However, the solution of the inverse problem is not unique and the choice of the reconstruction algorithm and other *a priori* assumptions influence the estimation of the dipoles resulting in potentially misleading results (Nolte *et al* 2004, Stam 2010, Stam *et al* 2006).

As an alternative to those two approaches, we apply $c(f)$ to groups of channels to characterize MEG background activity in AD and MCI. We want to study the spontaneous MEG in MCI and AD patients in contrast to elderly controls. $c(f)$ is computed from pairs of channels and the results are grouped attending at the location of channels over the scalp to estimate inter-regional coherence, likewise Stam *et al* (2006). Our results complement the intra-regional connectivity analysis by Alonso *et al* (2011), who analysed a smaller set of AD and control subjects by computing $c(f)$ and mutual information between pairs of channels in the same region. Their results suggested that AD is characterized by both decreases and increases of intra-regional connectivity in different frequency bands (Alonso *et al* 2011). We also introduce a novel methodology to extract the activity that simultaneously represents a group of channels. It relies on the adaptiveness of the empirical mode decomposition (EMD) (Huang *et al* 1998) and the ability of a constrained blind source separation (cBSS) (Lu and Rajapakse 2005) to extract brain activity. We hypothesize that this novel procedure could compute an adaptive regional extraction of signals with useful information about the brain activity. Actually, the EMD and cBSS have already been combined by Ye-Lin *et al* (2010) to denoise electroenterogram recordings. Their results support the usefulness of combining adaptive signal processing methodologies like EMD and blind source separation (BSS).

2. Subjects and MEG recordings

MEG signals were acquired from 80 subjects: 36 AD, 18 MCI and 26 control subjects. Clinical diagnosis was ascertained with exhaustive medical, neurological, psychiatric, neuroimaging (SPECT and MRI) and neuropsychological examinations. The mini-mental state examination (MMSE) (Folstein *et al* 1975) and the global deterioration scale/functional assessment staging (GDS/FAST) (Reisberg 1988) were used to screen the cognitive and functional status, respectively. All controls and patients' caregivers gave informed consent for participation in the study, which was approved by the local Ethics Committee.

The 36 AD patients (12 males and 24 females) fulfilled the criteria for probable AD according to the guidelines of the National Institute of Neurological of Communicative Disorders and Stroke—AD and Related Disorders Association (NINCDS–ADRDA) (McKhann *et al* 1984). Their mean age was 74.06 $\pm$ 6.95 years (mean $\pm$ standard deviation, SD) and the average scores in the cognitive and functional tests were 18.06 $\pm$ 3.36 for MMSE and 4.17 $\pm$ 0.45 for GDS/FAST (mean $\pm$ SD).

The MCI group was formed by 18 subjects (8 males and 10 females; age = 74.89 $\pm$ 5.57 years, mean $\pm$ SD) diagnosed following the Petersen's criteria (Petersen *et al* 2001). Two of them were categorized as amnesic MCI, while the others were included in the multiple-

domain category. The MCI patients' MMSE score was 25.67 ± 1.81 (mean ± SD) and all of them scored 3 in the GDS/FAST test.

Finally, 26 elderly control subjects (9 males and 17 females; age = 71.77 ± 6.38 years, mean ± SD) also participated in this study. The MMSE and GDS/FAST scores for the control group were 28.88 ± 1.18 and 1.73 ± 0.45 (mean ± SD), respectively. The difference in the mean age of the groups (both pairwise and when all three groups were simultaneously considered) was not statistically significant (in all cases $p > 0.10$, Student's t-test). Patients and control subjects were free of significant neurologic and psychiatric diseases other than AD or MCI. None of them was taking medication that could affect the MEG activity.

The MEG recordings were acquired using a 148-channel whole-head magnetometer (MAGNES 2500 WH, 4D Neuroimaging) located in a magnetically shielded room at the 'Centro de Magnetoencefalografía Dr Pérez-Modrego', Spain. The MEGs were recorded whilst the subjects lay on a hospital bed in a relaxed state, awake and with eyes closed. For each subject, 5 min of MEG background activity was recorded at 678.19 Hz with a 0.1–200 Hz hardware bandpass filter. The MEG equipment decimated each 5 min dataset by a factor of 4 as a trade-off between data length reduction and accurate representation of the δ, θ, α and β bands. This process consisted of filtering the data to avoid aliasing and downsampling the recordings. This anti-aliasing filter was a second-order Butterworth IIR filter with cut-off frequency at 76.30 Hz (45% of the final sample rate: 169.55 Hz), which was applied to the signals in both forward and reverse directions to avoid net phase shift. Per subject, 17.25 ± 6.47 (mean ± SD) epochs of 10 s (1695 samples) with minimal ocular activity were visually selected for analysis by an expert unaware of the subjects' clinical situation with the aid of an amplitude thresholding method (Hornero *et al* 2008).

Finally, in order to avoid biasing the computation of $c(f)$, the cardiac artefact was removed from the recordings with a cBSS-based procedure since this artefact can seriously affect the MEGs (Dammers *et al* 2008, Escudero *et al* 2007, Escudero *et al* 2011, James and Gibson 2003). We used the average of all MEG channels as a reference of the cardiac activity in each epoch (Escudero *et al* 2011). This average emphasizes the cardiac artefact, whereas the MEG background activity tends to cancel out as the cardiac artefact affects all channels simultaneously (Escudero *et al* 2011, 2007). Thus, the cardiac artefact could be enhanced in the average of the MEG channels (Escudero *et al* 2011, 2007). Then, an ECG-like template was derived from this average to guide a cBSS-based artefact removal (Escudero *et al* 2011). For the interested reader, alternative BSS-based procedures to remove the cardiac activity are also available elsewhere. For instance, Sander *et al* (2007) combined spectral, topographical and temporal features to identify the cardiac activity, while Dammers *et al* (2008) relied on amplitude and phase statistics to recognize and remove this artefact. Some cardiac artefact removal methods have been compared by Escudero *et al* (2011). The artefact-removed MEG signals were the input for both approaches used in the inter-regional connectivity assessment. For the sake of illustration, an MEG epoch recorded in the right posterior scalp region after the removal of the cardiac artefact is shown in figure 1 for a control, MCI and AD subject.

3. Methods

3.1. Overview

MEG recordings are composed of numerous channels and it may be helpful to group them into regions (Alonso *et al* 2011, Poza *et al* 2008, Stam *et al* 2006). In this study, the channels are grouped into left central (LC), anterior (LA), lateral (LL) and posterior (LP); and right

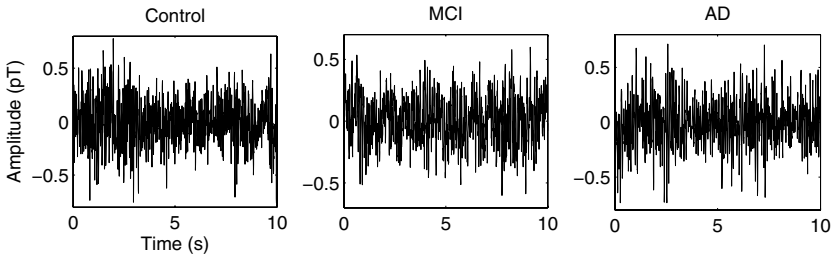

Figure 1. MEG signals recorded at channel 62, which is located in the right posterior region, for a control, MCI subject and AD patient. Amplitude and time are given in picotesla (pT) and second (s) units, respectively.

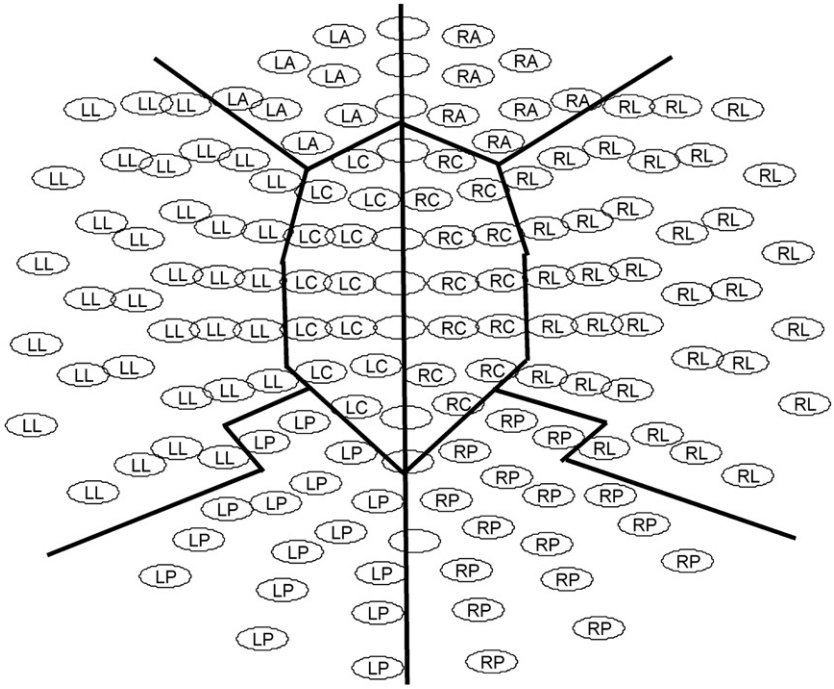

Figure 2. Distribution of the MEG sensors into left central (LC), anterior (LA), lateral (LL) and posterior (LP); and right central (RC), anterior (RA), lateral (RL) and posterior (RP) regions. Mid-line sensors appear empty. The lines depict the region boundaries.

central (RC), anterior (RA), lateral (RL) and posterior (RP) regions as shown in figure 2. This distribution is similar to that by Alonso *et al* (2011) and Poza *et al* (2008), but it also considers the difference between left and right channels. Mid-line sensors are not considered (Stam *et al* 2006).

$c(f)$ is computed with two different approaches. The first one consists of calculating $c(f)$ for all pairs of channels (Stam *et al* 2006), resulting in a large number of pairwise values. Then, the results are averaged considering the region to which each channel belongs (see figure 2) to estimate the inter-regional $c(f)$ in δ (1–4 Hz), θ (4–8 Hz), α (8–13 Hz) and β (13–30 Hz) bands.

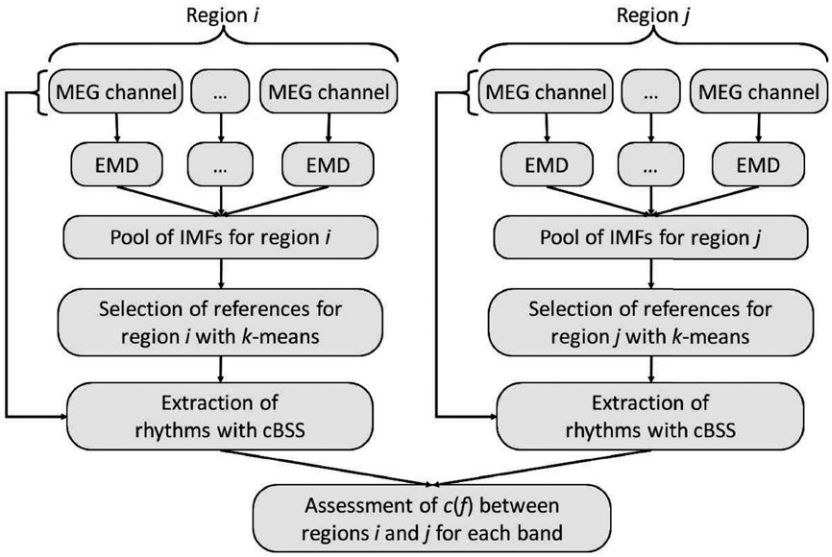

Figure 3. Block diagram of the processing steps included in the second approach to adaptively extract brain activity from each region and compute the $c(f)$ values.

In the second approach, the MEG inter-regional $c(f)$ is assessed by means of a novel adaptive procedure to characterize each region and band with a single signal. This approach is illustrated in figure 3, where the MEG channels appear on top of the diagram. An EMD is applied to each single channel to obtain the intrinsic mode functions (IMFs) (Huang *et al* 1998). Afterwards, all IMFs from channels in the same scalp region are combined into a 'pool' of single-channel rhythms. Subsequently, a *k*-means clustering (Hartigan and Wong 1979) is used to automatically select reference signals representative of the δ, θ, α and β bands from the pool of IMFs. Then, these references guide a cBSS (Lu and Rajapakse 2005) to extract one activity signal that simultaneously characterizes all channels in the region for every band. Finally, $c(f)$ is calculated between extracted signals of different regions to assess the connectivity.

3.2. Magnitude squared coherence—$c(f)$

$c(f)$ is used to measure brain synchrony (Dauwels *et al* 2010, Pereda *et al* 2005). It quantifies linear correlations as a function of frequency. $c(f)$ is bounded between 0 and 1. This measure can detect the linear synchronization between two signals, but it does not discriminate the directionality of the coupling (Dauwels *et al* 2010, Pereda *et al* 2005, Supp *et al* 2007). EEG experiments suggest that $c(f)$ is strongly correlated with other commonly used synchronization measures (Dauwels *et al* 2010).

First of all, two time series of equal length—$x(t)$ and $y(t)$—are divided into B equal blocks of 1 s each with 50% overlap. This block length was selected on the basis of the analyses by Dauwels *et al* (2010) to estimate the optimum parameters for a $c(f)$ computation similar to our first approach. $c(f)$ is calculated as (Alonso *et al* 2011, Dauwels *et al* 2010)

$$c(f) = \frac{|\langle X(f)Y^*(f)\rangle|^2}{|\langle X(f)\rangle||\langle Y(f)\rangle|}, \tag{1}$$

where $X(f)$ and $Y(f)$ are the Fourier transforms of $x(t)$ and $y(t)$, respectively, and * is the symbol for complex conjugate. Here, $|\cdot|$ denotes magnitude and $\langle\cdot\rangle$ indicates average over the B blocks (Alonso *et al* 2011, Dauwels *et al* 2010).

3.3. Adaptive extraction

This section describes a novel methodology to adaptively extract the brain activity from subsets of channels. This procedure is illustrated in figure 3 and applied to the regions depicted in figure 2. It relies on data-driven signal processing techniques such as EMD (Huang *et al* 1998), cBSS (Lu and Rajapakse 2005) and, to a lesser degree, k-means clustering (Hartigan and Wong 1979). These techniques are represented in the second, fifth and fourth rows of the diagram in figure 3, respectively.

3.3.1. Empirical mode decomposition. The EMD (Huang *et al* 1998) is a technique to adaptively represent non-stationary complex signals as a sum of their oscillations (i.e. IMFs). The EMD considers the oscillations in signals so that each IMF satisfies two basic conditions (Huang *et al* 1998).

- In each IMF time series, the number of extrema and the number of zero crossings must be the same or differ, at most, by 1.
- At any point, the mean value of the two envelopes defined by the local maxima and minima is 0.

Hence, the IMFs of a unidimensional signal $x(t)$ are calculated as follows (Flandrin *et al* 2004).

(i) Set $g_p(t) = x(t)$, with p the index of the extraction.
(ii) Detect the extrema (both maxima and minima) of $g_p(t)$.
(iii) Generate the upper and lower envelopes, $e_u(t)$ and $e_l(t)$, respectively, by connecting the maxima and minima separately with cubic spline interpolations.
(iv) The local mean, $m(t)$, is determined as $m(t) = [e_u(t) + e_l(t)]/2$.
(v) The IMF should have zero local mean. Thus, subtract $m(t)$ from the signal $g_p(t) \leftarrow [g_p(t) - m(t)]$.
(vi) Decide whether $g_p(t)$ is already an IMF by checking the two basic conditions described above. Otherwise, repeat steps ii–vi.

When the first IMF is derived ($p = 1$), set $d_p(t) = g_p(t)$, which is the smallest temporal scale (highest frequencies) in $x(t)$ (Flandrin *et al* 2004). In order to find the remaining IMFs, generate the residue $r_p(t)$ of the data by subtracting $d_p(t)$ from the signal as $r_p(t) = [x(t) - d_p(t)]$ (Flandrin *et al* 2004). Then, $r_p(t)$ is considered as the new data and subjected to the same sifting process described above (Flandrin *et al* 2004). The sifting process is continued until the final residue is a constant, a monotonic function or a function with one maxima and one minima from which no more IMFs can be derived (Flandrin *et al* 2004, Rilling *et al* 2003).

After the EMD, the unidimensional signal $x(t)$ is represented as

$$x(t) = \sum_{p=1}^{M} d_p(t) + r_M(t), \tag{2}$$

where M is the number of IMFs and $r_M(t)$ is the final residue (Huang *et al* 1998).

3.3.2. Frequency characterization of the IMFs. The EMD is applied to each single channel, as represented on top of figure 3, to isolate its oscillations. Then, the spectral content of each IMF has to be characterized. In order to do so, the instantaneous frequency of each IMF, $\omega_p(t)$, is computed as (Huang *et al* 1998)

$$\omega_p(t) = \frac{\mathrm{d}\theta_p(t)}{\mathrm{d}t}, \tag{3}$$

where $\theta_p(t)$ denotes the phase of the analytic signal, $z_p(t) = a_p(t)\exp[i\theta_p(t)] = d_p(t) + i\mathcal{H}[d_p(t)]$, computed from each IMF by means of the Hilbert transform $\mathcal{H}[\cdot]$ (Huang *et al* 1998).

Afterwards, a weighted average of the instantaneous frequency, $\overline{\omega}_p$, is computed from each $\omega_p(t)$ considering the amplitude

$$\overline{\omega}_p = \frac{E\{a_p(t)\omega_p(t)\}}{E\{a_p(t)\}}, \tag{4}$$

where $E\{\cdot\}$ refers to expectation. $\overline{\omega}_p$ contains the typical frequency of each IMF. Therefore, it characterizes its spectral content.

3.3.3. Reference selection. The IMFs represent oscillations in a single channel but they do not account for the rhythmic activity of a whole region. Therefore, a cBSS (Huang and Mi 2007, Lu and Rajapakse 2005) is used to extract the brain activity corresponding to a particular subset of channels for a specific frequency band (δ, θ, α and β). The cBSS needs a suitable reference (Huang and Mi 2007, James and Gibson 2003). This reference was selected with a k-means clustering.

The k-means algorithm is an effective and simple clustering procedure and it is appealing for its adaptive nature (Hartigan and Wong 1979). The algorithm divides a set of features (the $\overline{\omega}_p$ values) into k clusters automatically without any supervision (Hartigan and Wong 1979). After the initialization, the k-means clustering assigns the data values to the closest cluster centre. Then, the geometric centre of each cluster is recomputed, meaning that the clusters are recalculated. These steps are repeated until convergence is reached (Hartigan and Wong 1979).

For each region, all IMFs whose $\overline{\omega}_p$ value belongs to the broadband of interest (1–30 Hz) are aggregated into a 'pool' (see the third row of figure 3). Then, these $\overline{\omega}_p$ are fed into a k-means clustering initialized with four centroids in the middle of the spectral bands. Once convergence has been reached, the IMF corresponding with the closest $\overline{\omega}_p$ to each cluster's centroid is chosen as the reference for the cBSS applied to the channels from that region. This process is shown in the fourth row of figure 3.

3.3.4. Regional extraction of brain activity with cBSS. A reference per region and band is selected with k-means for being representative of the spectral location of the δ, θ, α or β band. Yet, this reference is indeed an IMF, which has been isolated from a single MEG channel. Hence, it is only representative of that channel. This reference will guide a cBSS to extract common activity representative for the whole region.

In general, BSS techniques estimate a set of n underlying unknown components—$\mathbf{s}(t) = [s_1(t), \ldots, s_n(t)]^T$—and the mixing matrix—$\mathbf{A}$—that generated a set of n observed recordings—$\mathbf{x}(t) = [x_1(t), \ldots, x_n(t)]^T$—through

$$\mathbf{x}(t) = \mathbf{A}\mathbf{s}(t). \tag{5}$$

The basic assumption in BSS is that the sources, also known as components, are statistically independent (Escudero *et al* 2009, James and Hesse 2005). An additive noise term can be included in the model to account for the lack of fit. The cBSS methods incorporate additional information into the separations so that the extracted component bears some relationship to a given reference (James and Hesse 2005).

Diverse implementations of the cBSS have been proposed (Huang and Mi 2007, Lu and Rajapakse 2005). Usually, the cBSS introduces a regularization parameter into a general-purpose BSS algorithm (Huang and Mi 2007, Lu and Rajapakse 2005). In this way, the cBSS obtains the statistically independent component that is closest to the reference (James and Gibson 2003). This reference only needs to be similar enough to drive the cBSS towards the desired component (James and Gibson 2003).

In this study, the algorithm by Huang and Mi (2007), which improves the method by Lu and Rajapakse (2005), has been used. The reference for the cBSS is the sign function of the IMF selected by the clustering (Huang and Mi 2007, James and Gibson 2003). The sign function was applied because the reference signal for the cBSS is most often constructed as a set of on/off pulses that guide the extraction of the components of interest (Huang and Mi 2007, James and Gibson 2003, James and Hesse 2005, Lu and Rajapakse 2005). Finally, once the brain activity is extracted for each band and region, $c(f)$ is computed. This procedure is illustrated in figure 3 by the presentation to the block that computes the $c(f)$ of the activities extracted for two different regions.

4. Results

4.1. Overview

After reducing the cardiac artefact, brain connectivity was computed with two different approaches. In the first one, $c(f)$ was calculated for all pairs of channels and the results are averaged accordingly to pairs of regions (Stam *et al* 2006). The second approach relied on the steps shown in figure 3. Illustrative examples of the outputs at key stages of this approach are given as follows.

First of all, an EMD is applied to each single MEG channel to estimate its oscillatory patterns. Figure 4 depicts the IMFs calculated from the control subject's MEG epoch plotted in figure 1. It can be seen that the spectral content of the rhythms moves from fast to slow frequencies as more IMFs are computed.

Secondly, each IMF is characterized with its $\overline{\omega}_p$ and a pool of IMFs from the same region is created. Then, k-means is applied to find the IMFs whose $\overline{\omega}_p$ values are the most representative (i.e. central) of the δ, θ, α and β bands. This process is exemplified in figure 5 for the IMFs of the same subject and region as figure 4. Figure 5 indicates the number of IMFs that have a particular value of $\overline{\omega}_p$ in the y axis. The vertical lines represent the centroid of each cluster.

Finally, once the reference for each region and band has been selected, the cBSS extracts the dominant activity in the band of interest for the region under consideration. All MEG channels from a region, together with the reference IMF selected by k-means, are fed to the cBSS. Then, the cBSS extracts a component that is statistically independent from the rest of the activity and similar to the reference. This computation is represented in figure 6 for the α band of the same subject and region as in figure 5.

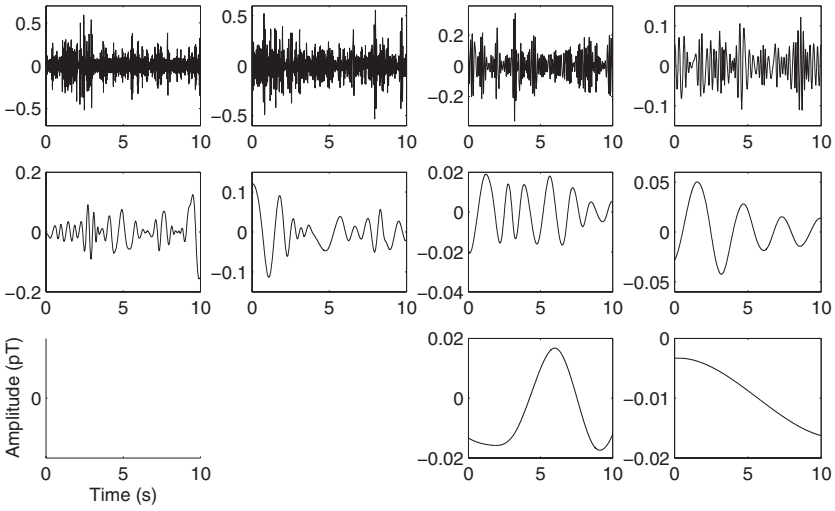

Figure 4. IMFs obtained from the control subject's MEG channel depicted in figure 1 plotted following their order of extraction from left to right and top to bottom.

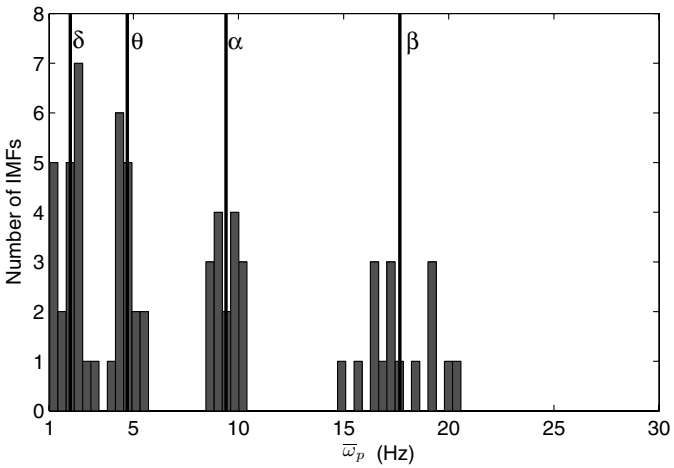

Figure 5. Reference selection with *k*-means applied to the RP region in the same control subject's MEG epoch as in figure 1. The four vertical lines indicate the position of the centroids for δ, θ, α and β.

In both approaches, the results were averaged for all MEG epochs so that the value of $c(f)$ per band, pair of regions and subject was obtained. It must be noted that the $c(f)$ values correspond to inter-regional, probably long-distance, brain connectivity.

4.2. Descriptive statistical analysis

Qualitative statistical analysis was performed to gain insight into the $c(f)$ values of AD, MCI and control subjects. Firstly, a repeated-measures ANalysis Of VAriance (ANOVA) was performed with the Greenhouse-Geisser correction for the lack of sphericity. The group (AD

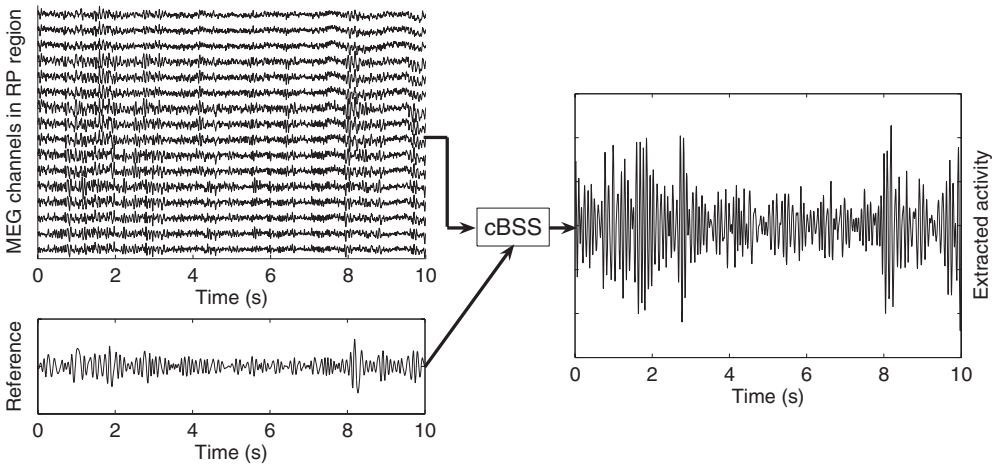

Figure 6. Illustration of the cBSS procedure for the α band in the RP region and for the same control subject's MEG epoch as in figure 1.

versus MCI versus controls) was the inter-subject factor, while the variables 'Band' (δ, θ, α and β) and 'Pair of regions' were taken as intra-subject factors. For the first approach, the ANOVA reported significant effects involving the factors 'Band', 'Pair' and their interaction ($p < 0.0001$). On the other hand, the inter-subject factor ('Diagnosis') was not significant ($p = 0.1015$). In the case of the EMD and cBSS approach, the effects of 'Band' ($p = 0.0132$), 'Pair' and 'Band×Pair' ($p < 0.0001$) were also significant. The effect of 'Diagnosis' was not significant ($p = 0.7005$) when all bands and pairs were simultaneously considered in the ANOVA.

A repeated-measures ANOVA (Greenhouse-Geisser correction) was applied to every band with 'Pair of regions' as the only intra-subject factor. For both approaches and all bands, there was a significant effect due to 'Pair of regions'. The level of $c(f)$ depended on the distance between the regions—e.g., the overall $c(f)$ level between regions located over the same hemisphere was usually higher than for pairs of left and right regions. 'Diagnosis' only had a significant effect for the δ band in the first approach ($p = 0.0100$).

In order to further explore the results, we inspected the estimated marginal means for the three subject groups for each band and approach. Figure 7 depicts these estimated marginal means, which revealed slight differences in the overall levels of inter-regional $c(f)$ for each approach. The estimated marginal means suggest that AD increases the level of $c(f)$ in the δ band while, MCI subjects tends to have lower connectivity in θ. The results in the upper bands are not conclusive, but a slight reduction in α inter-regional connectivity was found with the second approach. In addition, the estimated marginal means of $c(f)$ for the extracted brain activity were consistently lower than those values computed from the MEG channels (first approach).

4.3. Classification analysis

We also measured the ability of $c(f)$ to distinguish the groups in both approaches. A stepwise logistic regression with a full leave-one-out cross-validation (loo-cv) was applied to the $c(f)$ values from every band to classify the subjects into diagnosis pairs (controls versus MCI, controls versus AD and MCI versus AD). This procedure used all available subjects but one to

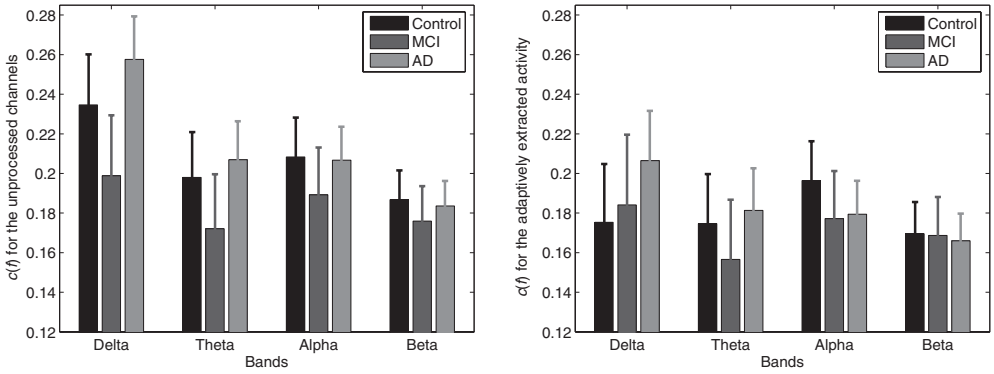

Figure 7. Estimated marginal means, with 95% confidence interval, of $c(f)$ from AD, MCI and control subjects in each spectral band for both approaches: (a) first approach, based on MEG channels, and (b) second approach, when EMD and cBSS were used for activity extraction.

Table 1. Pairwise stepwise logistic regression classification with a full loo-cv for the $c(f)$ computed from the MEG channels. The number of variables that were automatically selected in more than half the number of cases is also shown.

C versus M					
Band	δ	θ	α	β	Comb.
C correctly classified (%)	57.7	46.2	57.7	50.0	57.7
M correctly classified (%)	61.1	44.4	50.0	77.8	61.1
Global rate (%)	59.1	45.5	54.5	61.4	59.1
Commonly selected variables	1	1	3	1	1
C versus A					
C correctly classified (%)	42.3	69.2	53.8	42.3	46.2
A correctly classified (%)	36.1	55.6	55.6	44.4	55.6
Global rate (%)	38.7	61.3	54.8	43.5	51.6
Commonly selected variables	0	0	3	2	2
M versus A					
M correctly classified (%)	55.6	66.7	66.7	38.9	55.6
A correctly classified (%)	63.9	44.4	69.4	72.2	63.9
Global rate (%)	61.1	51.9	68.5	61.1	61.1
Commonly selected variables	1	1	2	0	2

C, M and A refer to controls, MCI and AD patients, respectively. 'Comb.' indicates that a combination of features of all bands was entered.

develop a classifier which was tested on the left-out subject. Then, this process was repeated for the other subjects. At every iteration, a forward stepwise variable selection was used to decide which variables would be included (if their associated $p < 0.05$) or removed (if $p > 0.10$) in the classifier. Tables 1 and 2 show the classification results based on $c(f)$ from the original MEG channels and from the extracted activity, respectively, as percentage of subjects correctly classified in each case (band and diagnoses).

Table 2. Pairwise stepwise logistic regression classification with a full loo-cv for the$c(f)$ of the adaptively extracted rhythms. The number of variables that were automatically selected in more than half the number of cases is also shown.

C versus M					
Band	δ	θ	α	β	Comb.
C correctly classified (%)	84.6	73.1	69.2	69.2	73.1
M correctly classified (%)	44.4	66.7	44.4	55.6	83.3
Global rate (%)	68.2	70.5	59.1	63.6	77.3
Commonly selected variables	2	1	1	3	4
C versus A					
C correctly classified (%)	69.2	50.0	53.8	84.6	84.6
A correctly classified (%)	69.4	47.2	75.0	47.2	58.3
Global rate (%)	69.4	48.4	66.1	62.9	69.4
Commonly selected variables	1	0	3	0	2
M versus A					
M correctly classified (%)	11.1	55.6	22.2	83.3	72.2
A correctly classified (%)	72.2	47.2	58.3	55.6	63.9
Global rate (%)	51.9	50.0	46.3	64.8	66.7
Commonly selected variables	2	1	0	2	2

C, M and A refer to controls, MCI and AD patients, respectively. 'Comb.' indicates that a combination of features of all bands was entered.

Tables 1 and 2 also display the number of variables that were included in the logistic regression in more than 50% of the iterations for every case. These consistently selected variables of individual bands were combined and the classification process repeated to check whether diverse spectral bands could have complementary information for the detection of MCI and AD. These results appear under the 'Comb.' headers in tables 1 and 2.

5. Discussion and conclusions

MEG background activity from 36 AD, 18 MCI and 26 control subjects was analysed to assess the MEG inter-regional connectivity with $c(f)$. Furthermore, a novel procedure to adaptively extract brain rhythmic activity from sets of channels was proposed. Hence, the aim of this study was twofold: to inspect the alterations that AD and MCI cause in the electromagnetic brain activity and to introduce a methodology based on EMD and cBSS to extract brain activity in δ, θ, α and β bands. The statistical analysis suggested that AD and MCI might affect the inter-regional connectivity, although the results were not statistically significant. However, a logistic regression with full loo-cv indicated that our methodology had higher accuracy in the classification of MCI and AD than computing $c(f)$ from the raw MEGs.

The cardiac contamination was reduced using a cBSS-based scheme (Escudero *et al* 2011, James and Gibson 2003). This ensured that the QRS complexes did not affect the IMFs that could serve as references to extract the rhythmic oscillations. Otherwise, the cardiac activity might have been present in some of the IMFs (Blanco-Velasco *et al* 2008), thus biasing the results. The same cardiac activity was estimated using the cBSS and removed from all MEG channels in order to avoid differences in the way the channels were preprocessed. This artefact removal was applied before any connectivity-related computation. Hence, the differences in

the results between both approaches cannot be due to that. Additionally, it is important to note that the MEG may suffer from baseline drifts or high-frequency noise. However, our analysis in the second approach is robust to the presence of these kinds of noise. Firstly, only frequencies between 1 and 30 Hz were considered in the calculation of $c(f)$. This spectral range includes the δ, θ, α and β bands while discarding the very low-frequency baseline drifts, whose spectrum is located below 1 Hz, and any high-frequency contamination over 30 Hz. Furthermore, the EMD isolates the high-frequency noise and the baseline drift in the first and last extracted IMFs, respectively. Since only the IMFs whose $\overline{\omega}_p$s are between 1 and 30 Hz are fed to the clustering process, the IMFs that account for baseline drift or high-frequency noise cannot be selected as references for the cBSS. Actually, the ability of the EMD to isolate baseline wanders and noise has been used to denoise biomedical recordings (Blanco-Velasco *et al* 2008).

Suitable references were selected among all IMFs from a region for each band. This procedure was carried out using a k-means clustering of the $\overline{\omega}_p$ values. Then, a cBSS was applied to simultaneously extract the activities from all channels in a region. This allowed us to consider the activity at the regional level, which is in contrast with processing single channels—'channel domain' (Alonso *et al* 2011, Gómez *et al* 2009b)—or localizing equivalent dipoles—'dipole domain' (Hoechstetter *et al* 2004, Rossini *et al* 2007, Supp *et al* 2007). Our approach is slightly similar to that adopted by Stam *et al* (2006), who carried out a channel-wise analysis and then grouped and averaged the results. Alternatively, we took a 'regional domain' approach and tested it on the classification of MCI and AD subjects. AD causes a slowdown and abnormalities in the nonlinear dynamics of the electromagnetic brain activity (Hornero *et al* 2009, Jeong 2004, Rossini *et al* 2007, Stam 2010). Although AD has been related to neocortical disconnection (Jeong 2004), this effect is not always easily detectable (Dauwels *et al* 2010). There is some consensus that AD decreases the synchronization level in high-frequency bands. Contradictory results have been found for low frequencies (Jeong 2004, Rossini *et al* 2007), but animal models suggest that acetylcholine loss decreases high-frequency EEG connectivity while increasing low-frequency coupling (Rossini *et al* 2007).

Although $c(f)$ only captures linear signal interactions (Gómez *et al* 2009b, Pereda *et al* 2005), it is not clear whether the alternative nonlinear connectivity measures are superior to $c(f)$ (Gómez *et al* 2009b). Moreover, the outcomes of $c(f)$ and other connectivity measurements seem to be correlated (Dauwels *et al* 2010). Diverse EEG studies have applied $c(f)$ to study MCI patients (Babiloni *et al* 2006, Dauwels *et al* 2010, Jeong 2004, Rossini *et al* 2006, 2007). It has been suggested that $c(f)$ might help to estimate the progression from MCI to AD (Rossini *et al* 2006). Yet, there are some divergences among studies, which might be due to differences in the analysed populations and the heterogeneity of MCI (Gómez *et al* 2009b).

The statistical analysis showed the clear dependences of $c(f)$ on the spectral band and pair of regions. The estimated marginal means supported the idea that AD decreases the connectivity of brain signals in α (Jeong 2004, Rossini *et al* 2007, Stam 2010). Moreover, they seemed to suggest that AD causes a rise in δ $c(f)$ levels. However, there were no significant differences between the groups. The fact that not all frequencies are equally affected by the changes in $c(f)$ indicates that the alterations are not simply due to a loss of cortical neurons (Dauwels *et al* 2010). Moreover, previous studies have reported opposite changes in different spectral bands in relation to AD (Alonso *et al* 2011, Stam *et al* 2009, van Cappellen van Walsum *et al* 2003). Actually, our results complement the intra-regional connectivity analysis by Alonso *et al* (2011), who reported an intra-regional increase in connectivity in low frequencies and a decrease in fast rhythms in a smaller sample of AD patients. The alterations

in connectivity might be due to anatomical disconnections among cortical regions or reduced cholinergic coupling between cortical neurons (Dauwels *et al* 2010).

A stepwise procedure automatically selected the most appropriate features from each single spectral band to classify the subjects at every single iteration of the loo-cv. This ensured that the development of the classifier (i.e. variable selection and training of the logistic regression) was not influenced at all by the testing data. We also evaluated the possible complementarity of features from diverse bands to diagnose the subjects. In these cases, only variables that had been frequently selected in single bands were presented to the classifier development. The aim was to avoid the over-fitting that would have appeared if all features from all bands (112 variables in total) had been used to classify a few dozens of subjects. The loo-cv reduces the accuracy levels but it avoids over-estimation of the true classification rates and increases the reproducibility of the results (Dauwels *et al* 2010). It must be noted that the number of variables selected by the stepwise procedure (with a maximum of 4) was small in comparison with the total number of features available for classification. Moreover, the combination of features from several bands tended to improve the performance of the classifier based on the $c(f)$ calculated with the proposed methodology.

Reported MEG-based classification rates of AD patients versus healthy elderly subjects usually are about 80% (Escudero *et al* 2009, Gómez *et al* 2009a, Hornero *et al* 2009, Poza *et al* 2008, Stam 2010). Our highest accuracies are relatively lower than those, but comparable to those found by Alonso *et al* (2011) in a smaller dataset. However, cross-validation techniques were not always applied in other papers. In this study, the accuracy reached 69.4% when variables of all bands were combined in the second approach to separate AD patients from controls.

The use of $c(f)$ features allowed us to classify MCI and control subjects with an accuracy of 77.3%. This value is lower than the accuracy obtained in an EEG study with neural networks (93.5%) (Rossini *et al* 2008) but close to that recently reported after an exhaustive EEG connectivity analysis (83%) (Dauwels *et al* 2010). However, care should be taken when comparing these results as different types of signals were studied. A difference of more than 12 years in the mean age of MCI and controls existed in the work by Rossini *et al* (2008), while the groups were matched in age in our study. Furthermore, our result compares favourably with a previous study that classified a similar dataset of MCI and controls with an accuracy of 69.8% without cross-validation (Gómez *et al* 2009b).

Rather than trying to estimate the equivalent current dipoles or computing $c(f)$ for pairs of channels, the activity was extracted at a regional level. It is important to note that the cBSS does not estimate equivalent current dipoles. Instead, it extracts a signal component that is independent from the rest of the brain activity and close to a reference (Huang and Mi 2007, James and Gibson 2003, Lu and Rajapakse 2005). This procedure allowed us to obtain the activity that jointly represents a set of channels (Lu and Rajapakse 2005). Thus, the extracted component accounts for the dominant activity in each of the bands of interest for every region. This novel approach led to two noticeable results. Firstly, the estimated marginal means tended to be lower when $c(f)$ was computed with the proposed methodology than when calculated from the raw MEG channels. Secondly, the adaptive extraction of activity used to provide higher classification accuracies than the MEG channels. A potential explanation for these two results might be that the extraction helped to reduce the impact of the contamination from other activities into the inter-regional connectivity. This might alleviate the volume conduction effect, which is stronger at nearby channels, and its associated bias in $c(f)$ (Nolte *et al* 2004, Stam *et al* 2009). Nevertheless, we do acknowledge that additional tests are needed to corroborate or refute this hypothetical explanation. Other limitations of this study also merit consideration. Firstly, the sample size is small to prove the usefulness

of our approach as a diagnostic tool. Thus, a larger database is needed to confirm the results. Secondly, and similar to other studies (Dauwels *et al* 2010), we mainly tried to help in the discrimination of subject groups. We did not aim at identifying the biophysical mechanisms that cause the alterations of AD and MCI in the MEGs. Finally, the subjects did not perform any specific task. Hence, the classification performance might be improved by analysing signals acquired during specific tasks (Dauwels *et al* 2010, Stam 2010).

To sum up, we have introduced a novel methodology to extract the activity from MEG scalp regions. We have also assessed the connectivity alterations caused by AD and MCI in the electromagnetic brain activity. Our results suggest that the proposed methodology could provide information about the connectivity pattern in MEG. Furthermore, they prove the usefulness of this procedure in the classification of AD and MCI patients versus healthy elderly subjects.

Acknowledgments

The authors would like to thank the 'Asociación de Familiares de Enfermos de Alzheimer' (Madrid, Spain) for providing the patients who participated in this study and Dr Alberto Fernández ('Centro de Magnetoencefalografía Dr Pérez-Modrego'), who collected the MEG recordings. They are also thankful to the Reviewers and the Editorial Office for their feedback about the manuscript. This work was supported in part by the Spanish 'Ministerio de Ciencia e Innovación' (Ref: TEC2008-02241) and by a Spanish FPU grant (Ref: AP2007-03303) awarded to J Escudero.

References

Abásolo D, Escudero J, Hornero R, Gómez C and Espino P 2008 Approximate entropy and auto mutual information analysis of the electroencephalogram in Alzheimer's disease patients *Med. Biol. Eng. Comput.* **46** 1019–28

Abatzoglou I, Anninos P, Adamopoulos A and Koukourakis M 2007 Nonlinear analysis of brain magnetoencephalographic activity in Alzheimer disease patients *Acta Neurol. Belg.* **107** 34–9

Abatzoglou I, Anninos P, Tsalafoutas I and Koukourakis M 2009 Multi-channel magnetoencephalogram on Alzheimer disease patients *J. Integr. Neurosci.* **8** 13–22

Alonso J, Poza J, Mañanas M, Romero S, Fernández A and Hornero R 2011 MEG connectivity analysis in patients with Alzheimer's disease using cross mutual information and spectral coherence *Ann. Biomed. Eng.* **39** 524–36

Babiloni C *et al* 2006 Fronto-parietal coupling of brain rhythms in mild cognitive impairment: a multicentric EEG study *Brain Res. Bull.* **69** 63–73

Blanco-Velasco M, Weng B and Barner K 2008 ECG signal denoising and baseline wander correction based on the empirical mode decomposition *Comput. Biol. Med.* **38** 1–13

Blennow K, de Leon M J and Zetterberg H 2006 Alzheimer's disease *Lancet* **368** 387–403

Dammers J, Schiek M, Boers F, Silex C, Zvyagintsev M, Pietrzyk U and Mathiak K 2008 Integration of amplitude and phase statistics for complete artifact removal in independent components of neuromagnetic recordings *IEEE Trans. Biomed. Eng.* **55** 2353–62

Dauwels J, Vialatte F, Musha T and Cichocki A 2010 A comparative study of synchrony measures for the early diagnosis of Alzheimer's disease based on EEG *Neuroimage* **49** 668–93

Escudero J, Hornero R, Abásolo D and Fernández A 2009 Blind source separation to enhance spectral and non-linear features of magnetoencephalogram recordings. Application to Alzheimer's disease *Med. Eng. Phys.* **31** 872–9

Escudero J, Hornero R, Abásolo D and Fernández A 2011 Quantitative evaluation of artifact removal in real magnetoencephalogram signals with blind source separation *Ann. Biomed. Eng.* at press

Escudero J, Hornero R, Abásolo D, Fernández A and López-Coronado M 2007 Artifact removal in magnetoencephalogram background activity with independent component analysis *IEEE Trans. Biomed. Eng.* **54** 1965–73

Fernández A, Hornero R, Mayo A, Poza J, Gil-Gregorio P and Ortiz T 2006 MEG spectral profile in Alzheimer's disease and mild cognitive impairment *Clin. Neurophysiol.* **117** 306–14

Ferri C P *et al* 2006 Global prevalence of dementia: a Delphi consensus study *Lancet* **366** 2112–7

Flandrin P, Rilling G and Gonçalvès P 2004 Empirical mode decomposition as a filter bank *IEEE Signal Process. Lett.* **11** 112–4

Folstein M, Folstein S and McHugh P 1975 Mini-mental state. A practical method for grading the cognitive state of patients for the clinician *J. Psychiatr. Res.* **12** 189–98

Gómez C, Hornero R, Abásolo D, Fernández A and Escudero J 2009a Analysis of MEG background activity in Alzheimer's disease using nonlinear methods and ANFIS *Ann. Biomed. Eng.* **37** 586–94

Gómez C, Stam C, Hornero R, Fernández A and Maestú F 2009b Disturbed beta band functional connectivity in patients with mild cognitive impairment: an MEG study *IEEE Trans. Biomed. Eng.* **56** 1683–90

Hartigan J A and Wong M A 1979 A k-means clustering algorithm *J. R. Stat. Soc.* C **28** 100–8

Hoechstetter K, Bornfleth H, Weckesser D, Ille N, Berg P and Scherg M 2004 BESA source coherence: a new method to study cortical oscillatory coupling *Brain Topogr.* **16** 233–8

Hornero R, Abásolo D, Escudero J and Gómez C 2009 Nonlinear analysis of electroencephalogram and magnetoencephalogram recordings in patients with Alzheimer's disease *Phil. Trans. R. Soc.* A **367** 317–36

Hornero R, Escudero J, Fernández A, Poza J and Gómez C 2008 Spectral and nonlinear analyses of MEG background activity in patients with Alzheimer's disease *IEEE Trans. Biomed. Eng.* **55** 1658–65

Huang D and Mi J 2007 A new constrained independent component analysis method *IEEE Trans. Neural Netw.* **18** 1532–5

Huang N, Shen Z, Long S, Wu M, Shih H, Zheng Q, Yen N, Tung C and Liu H 1998 The empirical mode decomposition and the Hilbert spectrum for nonlinear and non-stationary time series analysis *Proc. R. Soc.* A **454** 903–95

James C and Gibson O 2003 Temporally constrained ICA: an application to artifact rejection in electromagnetic brain signal analysis *IEEE Trans. Biomed. Eng.* **50** 1108–16

James C and Hesse C 2005 Independent component analysis for biomedical signals *Physiol. Meas.* **26** R15–39

Jeong J 2004 EEG dynamics in patients with Alzheimer's disease *Clin. Neurophysiol.* **115** 1490–505

Lu W and Rajapakse J 2005 Approach and applications of constrained ICA *IEEE Trans. Neural Netw.* **16** 203–12

McKhann G, Drachman D, Folstein M, Katzman R, Price D and Stadlan E 1984 Clinical diagnosis of Alzheimer's disease: report of the NINCDS-ADRDA Work Group under the auspices of Department of Health and Human Services Task Force on Alzheimer's Disease *Neurology* **34** 939–44

Nestor P J, Scheltens P and Hodges J R 2004 Advances in the early detection of Alzheimer's disease *Nat. Rev. Neurosci.* **5** (Suppl.) S34–41

Nolte G, Bai O, Wheaton L, Mari Z, Vorbach S and Hallett M 2004 Identifying true brain interaction from EEG data using the imaginary part of coherency *Clin. Neurophysiol.* **115** 2292–307

Pereda E, Quiroga R and Bhattacharya J 2005 Nonlinear multivariate analysis of neurophysiological signals *Prog. Neurobiol.* **77** 1–37

Petersen R C, Stevens J C, Ganguli M, Tangalos E G, Cummings J L and DeKosky S T 2001 Practice parameter: early detection of dementia: mild cognitive impairment (an evidence-based review): report of the Quality Standards Subcommittee of the American Academy of Neurology *Neurology* **56** 1133–42

Poza J, Hornero R, Escudero J, Fernández A and Sánchez C 2008 Regional analysis of spontaneous MEG rhythms in patients with Alzheimer's disease using spectral entropies *Ann. Biomed. Eng.* **36** 141–52

Reisberg B 1988 Functional assessment staging (FAST) *Psychopharmacol. Bull.* **24** 653–9

Rilling G, Flandrin P and Gonçalvès P 2003 On empirical mode decomposition and its algorithms *IEEE EURASIP Workshop on Nonlinear Signal and Image Processing NSIP-03 (Grado, Italy)*

Rossini P, Buscema M, Capriotti M, Grossi E, Rodriguez G, Del Percio C and Babiloni C 2008 Is it possible to automatically distinguish resting EEG data of normal elderly vs mild cognitive impairment subjects with high degree of accuracy? *Clin. Neurophysiol.* **119** 1534–45

Rossini P *et al* 2006 Conversion from mild cognitive impairment to Alzheimer's disease is predicted by sources and coherence of brain electroencephalography rhythms *Neuroscience* **143** 793–803

Rossini P, Rossi S, Babiloni C and Polich J 2007 Clinical neurophysiology of aging brain: from normal aging to neurodegeneration *Prog. Neurobiol.* **83** 375–400

Sander T, Burghoff M, Van Leeuwen P and Trahms L 2007 Application of decorrelation-independent component analysis to biomagnetic multi-channel measurements *Biomed. Tech.* **52** 130–6

Stam C 2010 Use of magnetoencephalography (MEG) to study functional brain networks in neurodegenerative disorders *J. Neurol. Sci.* **289** 128–34

Stam C *et al* 2009 Graph theoretical analysis of magnetoencephalographic functional connectivity in Alzheimer's disease *Brain* **132** 213–24

Stam C, Jones B, Manshanden I, van Cappellen van Walsum A, Montez T, Verbunt J, de Munck J, van Dijk B, Berendse H and Scheltens P 2006 Magnetoencephalographic evaluation of resting-state functional connectivity in Alzheimer's disease *Neuroimage* **32** 1335–44

Supp G, Schlögl A, Trujillo-Barreto N, Müller M and Gruber T 2007 Directed cortical information flow during human object recognition: analyzing induced EEG gamma-band responses in brain's source space *PLoS One* **2** e684

van Cappellen van Walsum A, Pijnenburg Y, Berendse H, van Dijk B, Knol D, Scheltens P and Stam C 2003 A neural complexity measure applied to MEG data in Alzheimer's disease *Clin. Neurophysiol.* **114** 1034–40

Ye-Lin Y, Garcia-Casado J, Prats-Boluda G and Martinez-de Juan J 2010 Combined method for reduction of high frequency interferences in surface electroenterogram (EEnG) *Ann. Biomed. Eng.* **38** 2358–70